Cerebral Cortex May 2009;19:1186-1197
doi:10.1093/cercor/bhn166
Advance Access publication September 26, 2008

Smooth Pursuit–Related Information Processing in Frontal Eye Field Neurons that Project to the NRTP

Seiji Ono and Michael J. Mustari

Division of Sensory-Motor Systems, Yerkes National Primate Research Center, and Department of Neurology, Emory University, 954 Gatewood Road Northeast, Atlanta, GA 30329, USA

The cortical pursuit system begins the process of transforming visual signals into commands for smooth pursuit (SP) eye movements. The frontal eye field (FEF), located in the fundus of arcuate sulcus, is known to play a role in SP and gaze pursuit movements. This role is supported, at least in part, by FEF projections to the rostral nucleus reticularis tegmenti pontis (rNRTP), which in turn projects heavily to the cerebellar vermis. However, the functional characteristics of SP-related FEF neurons that project to rNRTP have never been described. Therefore, we used microelectrical stimulation (ES) to deliver single pulses (50–200 μA, 200-μs duration) in rNRTP to antidromically activate FEF neurons. We estimated the eye or retinal error motion sensitivity (position, velocity, and acceleration) of FEF neurons during SP using multiple linear regression modeling. FEF neurons that projected to rNRTP were most sensitive to eye acceleration. In contrast, FEF neurons not activated following ES of rNRTP were often most sensitive to eye velocity. In similar modeling studies, we found that rNRTP neurons were also biased toward eye acceleration. Therefore, our results suggest that neurons in the FEF–rNRTP pathway carry signals that could play a primary role in initiation of SP.

Keywords: cerebral cortex, eye movements, macaque, pontine nucleus

Introduction

The primate visual system is specialized for central vision, which is served by the high-acuity region of the retina known as the fovea. To examine an object of interest in detail, its image must be located on or near the fovea. This is achieved by different oculomotor subsystems including fixation, vestibular ocular, optokinetic, saccadic, vergence, and smooth pursuit (SP) that maintain the image of the visual world or a selected target stable on the retina during movement of the observer (for review, see Leigh and Zee 2006). SP is a volitional activity supported by interconnected regions of cerebral cortex including middle temporal (MT), medial superior temporal (MST), lateral intraparietal, frontal eye field (FEF), and supplementary eye fields (SEFs). This network, known as the cortical pursuit system, is responsible for beginning the process of converting visual motion information into commands for eye movements (for review, see Krauzlis 2004). Each subregion of the cortical pursuit system has specialized properties related to different aspects of volitional SP and has complimentary patterns of cortico-cortical and cortico-brain stem projections. Our studies are directed at understanding information processing in FEF neurons that project to specific regions of the SP system.

The FEF region is located in association with the arcuate sulcus and contains saccade, vergence, and SP-related neurons (for review, see MacAvoy et al. 1991; Gottlieb et al. 1994; Fukushima 2003). SP-related FEF neurons are located mostly caudal to saccade-related neurons in the fundus of the arcuate sulcus (for review, see Fukushima 2003). The anatomical connections of the saccadic and SP regions of FEF with other areas of cortex and brain stem are mostly nonoverlapping (for review, see Lynch and Tian 2006). The FEF has reciprocal connections with MT and MST areas, which play important roles in visual motion processing appropriate for generation of initial pursuit commands (e.g., Maunsell and Newsome 1987; Komatsu and Wurtz 1988).

Lesions in the FEF of monkeys and humans result in a reduction of SP gain toward the side of lesion (ipsilesional) (Lynch 1987; Shi et al. 1988; Morrow and Sharpe 1990; Keating 1991, 1993; MacAvoy et al. 1991; Morrow 1996). Additionally, electrical stimulation of monkey FEF elicits slow continuous eye movements that are predominantly ipsilateral in direction (Bruce et al. 1985; Keller and Heinen 1991; MacAvoy et al. 1991; Gottlieb et al. 1993, 1994; Tian and Lynch 1996; Tanaka and Lisberger 2001). Single-unit recording studies show that FEF pursuit neurons have appropriate response properties to play a role in the initiation and maintenance of SP (MacAvoy et al. 1991; Gottlieb et al. 1994; Tanaka and Fukushima 1998; Tanaka and Lisberger 2002; Drew and van Donkelaar 2007). FEF neurons typically begin their discharge prior to the onset of SP and carry extraretinal signals related to volitional SP (for review, see Fukushima 2003; Ono and Mustari 2007).

For the cortical pursuit system and FEF per se to effect SP, signals must be delivered to appropriate brain stem centers including dorsolateral pontine nucleus (DLPN) and the nucleus reticularis tegmenti pontis (NRTP), which are known to play complimentary roles in SP (Ono et al. 2004, 2005). The DLPN and rostral NRTP (rNRTP) provide mossy fiber inputs to the floccular complex and oculomotor vermis (lobules VI and VII) of the cerebellum (Kunzle and Akert 1977; Brodal 1980, 1982; Huerta et al. 1986; Shook et al. 1990; Giolli et al. 2001; Distler et al. 2002; for review, see Thier and Möck 2006). These cerebellar areas are essential for controlling SP eye movements (see Discussion).

The functional characteristics of SP-related FEF neurons that actually project to rNRTP or elsewhere have never been described. Therefore, we used microelectrical stimulation (ES) delivered among SP-related rNRTP neurons to antidromically activate FEF neurons. This technique allows us to provide the most detailed information possible regarding signals sent by FEF neurons to a structure that is essential for SP (Suzuki et al. 1999, 2003; Ono et al. 2004, 2005)

Materials and Methods

Surgical Procedures

Two juvenile rhesus (*Macaca mulatta*) monkeys (3–5 years old, 5–8 kg), born in captivity at the Yerkes National Primate Research Center,

were used in this study. A detailed description of our surgical procedures can be found in earlier publications (e.g., Mustari et al. 2001; Ono and Mustari 2007). All surgical procedures were performed in compliance with National Institutes of Health Guide for the Care and Use of Laboratory Animals, and protocols were reviewed and approved by the Institutional Animal Care and Use Committee at Emory University. Surgical procedures were performed in a dedicated facility using aseptic techniques under isoflurane anesthesia (1.25–2.5%). Vital signs including blood pressure, heart rate, blood oxygenation, body temperature, and CO_2 in expired air were monitored with a Surgivet Instrument (Waukesha, WI) and maintained in normal physiological limits. Postsurgical analgesia (Buprenorphine 0.01 mg/kg, intramuscularly [i.m.]) and anti-inflammatory (Banamine 1.0 mg/kg, IM) treatment were delivered every 6 h for several days, as indicated. To permit single-unit recording, we used stereotaxic methods to implant a titanium head stabilization post and titanium recording chambers (Crist Instruments, Hagerstown, MD) over the FEF and pontine regions. In the same surgery, a scleral search coil for measuring eye movements (Fuchs and Robinson 1966) was implanted underneath the conjunctiva of one eye using the technique of Judge et al. (1980).

Localization of the FEF

We first located the FEF by its stereotaxic location (anterior = 22 mm, lateral = 20 mm) and by finding neurons that were modulated during SP of a small diameter (0.2°) target spot moving (±10°, 0.1–0.75 Hz) over a dark background. We further verified that our recording locations were in the FEF using magnetic resonance imaging (*T*1-weighted, fast spin echo; Siemens, 3-T magnet [Siemens, Princeton, NJ]) and electrode track depth measurements taken from microdrive readings while recording SP neurons in FEF (Fig. 1*A*). The location of our SP neurons in the fundus of the arcuate sulcus was similar to that reported by other investigators (e.g., Tanaka and Fukushima 1998).

Behavioral Paradigms

During all experiments, monkeys were seated in a primate chair (Crist Instruments) with the head stabilized in the horizontal stereotaxic plane. Experiments were conducted in a sound-attenuated and lightproof room. Visual stimuli were rear projected on a tangent screen 57 cm distant from the monkey. SP targets were delivered using appropriate optic bench hardware and computer-controlled 2-axis mirror galvanometers (General Scanning, Watertown, MA) as described in detail in previous publications (e.g., Mustari et al. 2001; Ono et al. 2004). Neurons in the FEF that responded during SP of a small diameter (0.2°) target spot moving at low frequency (0.1–0.75 Hz, ±10°) were included in this study. Neurons were tested while the monkey tracked a small target that moved in 1 of 8 cardinal directions separated by 45°. Once we found the best direction for pursuit, we tested several different speeds (10–30°/s) in the preferred direction. We used the speed associated with maximum sensitivity of the neuron in further testing and analysis. FEF neurons that showed only static eye position sensitivity were not categorized as SP neurons and were not included in modeling studies. All neurons were tested as monkeys tracked a target spot that moved with a step-ramp trajectory over dark background. The size of the step was adjusted so that the monkey initiated SP eye without early saccadic intrusions (Rashbass 1961). Usually the size of the step was between 2 and 4 degrees. Data collected during step-ramp testing were used for the model-fitting procedures described below. We included step-ramp trials where the target was briefly extinguished to reveal extraretinal signals (see below).

Data Collection

Eye movements were detected and calibrated using standard electromagnetic methods (Fuchs and Robinson 1966) using precision hardware (CNC Electronics, Seattle, WA). Eye and target position feedback signals were processed with anti-aliasing filters at 200 Hz using 6-pole Bessel filters prior to digitization at 1 kHz with 16-bit precision. Velocity data were generated by digital differentiation of position data using a central difference algorithm in Matlab (Mathworks, Natick, MA). Single-unit activity was recorded from FEF using modified commercial epoxy-coated tungsten (Frederick-Haer Corporation, Brunswick, ME). The impedance of the electrodes was in the 1- to 3-MOhm range. Single-unit action potentials were detected with either a window discriminator (Bak Electronics, Mount Airy, MD) or a template matching algorithm (Alpha-Omega, Alpharetta, GA) and represented by a transistor-transistor logic (TTL) pulse, which was sampled at high precision as an event mark in our data acquisition system (CED Power1401, Cambridge, UK). During analysis, neuronal response was represented as a spike density function that was generated by convolving spike times with a 5-ms Gaussian function (Richmond et al. 1987).

Electrical Stimulation of rNRTP

We implanted the brain stem chamber in the coronal stereotaxic plane, 3 mm anterior to earbar zero, and with a 20° lateral tilt (e.g., Ono et al. 2004, 2005). To accurately locate the rNRTP region, we first mapped the anatomical midline by finding the oculomotor neurons with characteristic burst-tonic firing patterns during saccades with either rightward or leftward on directions. Next, we localized the rNRTP by its stereotaxic location 5- to 7-mm deep to the oculomotor nucleus (OMN) and by finding neurons that were modulated during SP of a small diameter (0.2°) target spot moving (±10°, 0.1–0.75 Hz) over a dark background. We verified that our recording locations were in the NRTP by using magnetic resonance imaging (T_1-weighted, fast spin echo; Siemens, 3-T magnet) and Nissl-stained sections (e.g., Ono et al. 2004). The sites of our SP-related neurons in rNRTP are consistent with those reported in previous studies that included histological reconstruction of recording sites (Suzuki et al. 2003; Ono et al. 2004; 2005).

We then attempted to antidromically activate each FEF neuron recorded by delivering single biphasic ES pulses (10–200 μA, 200-μs duration) in rNRTP (Fig. 1*B*). Activation thresholds for FEF neurons ranged from 20 to 200 μA and occurred at short latency (Fig. 1*C*). We did not use higher currents because we wanted to limit spread of current to surrounding structures (see below). A FEF neuron was considered antidromically activated if it discharged at a constant latency after each ES pulse (Fig. 1*B*, top) and passed the collision test. In Figure 1*B*, we show typical results of this testing by superimposing 5 successive repetitions in each condition. The mean action potential duration of our antidromically activated FEF projection neurons was 331 μs (standard deviation = 103 μs, n = 20). Such relatively long-duration action potentials fall in range similar to that reported for cortical projection neurons in other systems (for review, see Mitchell et al. 2007). The FEF spikes produced or expected following electrical stimulation of rNRTP are indicated with asterisks (Fig. 1*B*). We used collision testing to verify that the spike evoked by electrical stimulation was due to antidromic rather than orthodromic activation. For collision testing, we used a naturally occurring spike from a well-isolated FEF neuron (Fig. 1*D*) to trigger the pulse generator (CED power 1401) at variable delays (Fig. 1*B*, middle and bottom). For collision testing, we always used a TTL pulse generated by a hardware window discriminator (Bak Electronics) to represent time of occurrence of the well-isolated spike. We could control the time separation between the natural FEF spike and electrical stimulation pulse in 0.1-ms increments until we found a time separation (Fig. 1*B*, appropriate timing) that resulted in failure to evoke a spike by electrical stimulation (i.e., collision point; Fig. 1*B*, bottom). We constrained the electrical stimulation so that at least 1 s was allowed before a subsequent stimulus pulse was delivered.

We were able to verify that our low-current stimulus pulse selectively activated FEF axons in the rNRTP and not surrounding structures. We did this by attempting to activate the FEF neurons a short distance (200–500 μm) above the NRTP per se. Figure 2 shows an example of this testing. We show a histological reconstruction of our recording sites taken from a Nissl-stained section (left panel). We indicate the anatomical location of the rNRTP and successful recording sites (filled circles) in the line drawings taken from the Nissl-stained section. Electrode tracks can be seen traveling to both the left and the right rNRTPs. We stimulated the right rNRTP to antidromically activate neurons in the right FEF. In the right panel of Figure 2, we show that we were able to antidromically activate FEF neurons (asterisk) when stimuli were delivered in the rNRTP but not when the pulses were delivered a short distance (500 μm) above the rNRTP. In this study, we

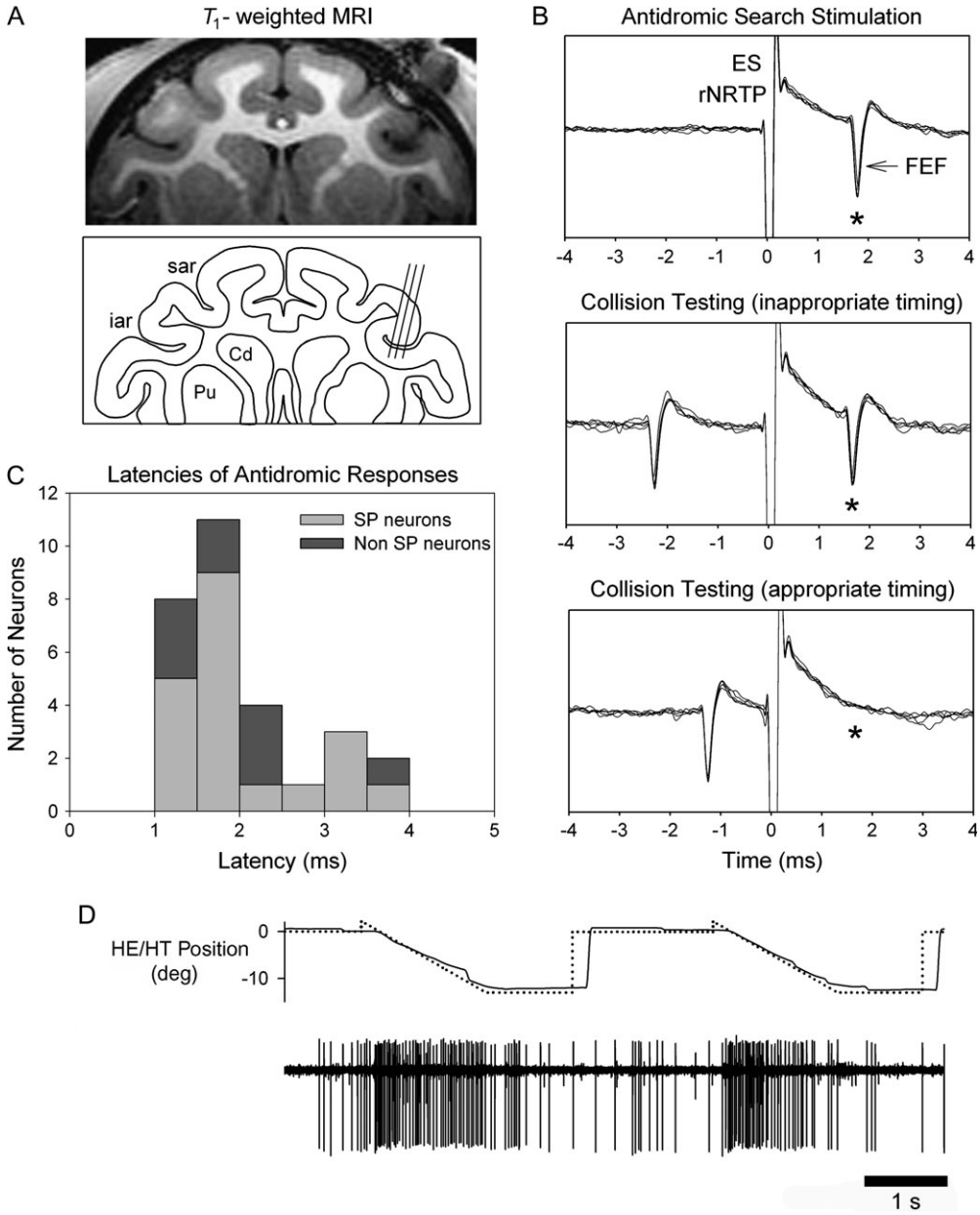

Figure 1. Location of FEF and examples of unit testing during SP. (*A*) Recoding sites of SP neurons in right FEF verified by structural magnetic resonance imaging (MRI) (T_1-weighted, fast spin echo; Siemens, 3-T magnet). Line drawing indicating representative recording tracks run on a 15° angle tilted lateral with respect to pure vertical. Penetrations and unit depths reconstructed by MRI and measurements taken from microdrive readings during recording SP neurons in FEF. (*B*) SP-related FEF neuron antidromically activated (*) following biphasic single-pulse electrical stimulation (50 μA, 200-μs duration) of the rNRTP at the depth of SP neurons. Top panel: 5 successive antidromic trials in "search mode" aligned on the electrical stimulation artifact. Middle panel: antidromic spikes (*) continue to be elicited when inappropriate timing was used between a naturally occurring FEF spike and the stimulus pulse. Bottom panel: when appropriate timing is used between the naturally occurring spike and the stimulus pulse collision occurs (i.e., no evoked FEF at expected time (*). (*C*) Histogram of latencies between onset of electrical stimulation pulse in rNRTP and evoked FEF spikes. Median latency between stimulation in the rNRTP and evoked FEF spikes was 1.69 ms. Mean action potential duration of antidromically activated FEF neurons was 331 μs (standard deviation = 103 μs). (*D*) Representative well-isolated FEF neuron during 2 successive step-ramp trials.

did not attempt to activate FEF neurons from other basilar pontine sites (see Discussion).

Model Fitting and Optimization

FEF neurons evince sensitivity to eye and visual motion per se (Fig. 3). Figure 3*A* shows an example of a FEF neuron tested during SP where the target was briefly extinguished to reveal extraretinal sensitivity, as reported by other investigators (Tanaka and Fukushima 1998). Figure 3*B* shows a representative FEF neuron tested during sinusoidal SP and during fixation with visual stimulation. In this testing, either a small target spot (Fig. 3*B*, left) or a large-field visual stimulus (Fig. 3*B*, right) was moved in a direction and speed like that used during SP eye movements. These types of visual stimuli produced direction-selective modulation of neuronal firing (see Discussion). In Figure 3*C*, we show the distribution of FEF neurons in our sample with sensitivity to both eye motion and large-field visual motion. At least 60% of our antidromically activated FEF neurons had explicit visual and eye motion sensitivity. These results argue for inclusion of eye and retinal image motion parameters in our modeling studies (see Discussion).

We used a model estimation procedure to identify SP-related signals in FEF during step-ramp tracking. We attempted to reconstruct the

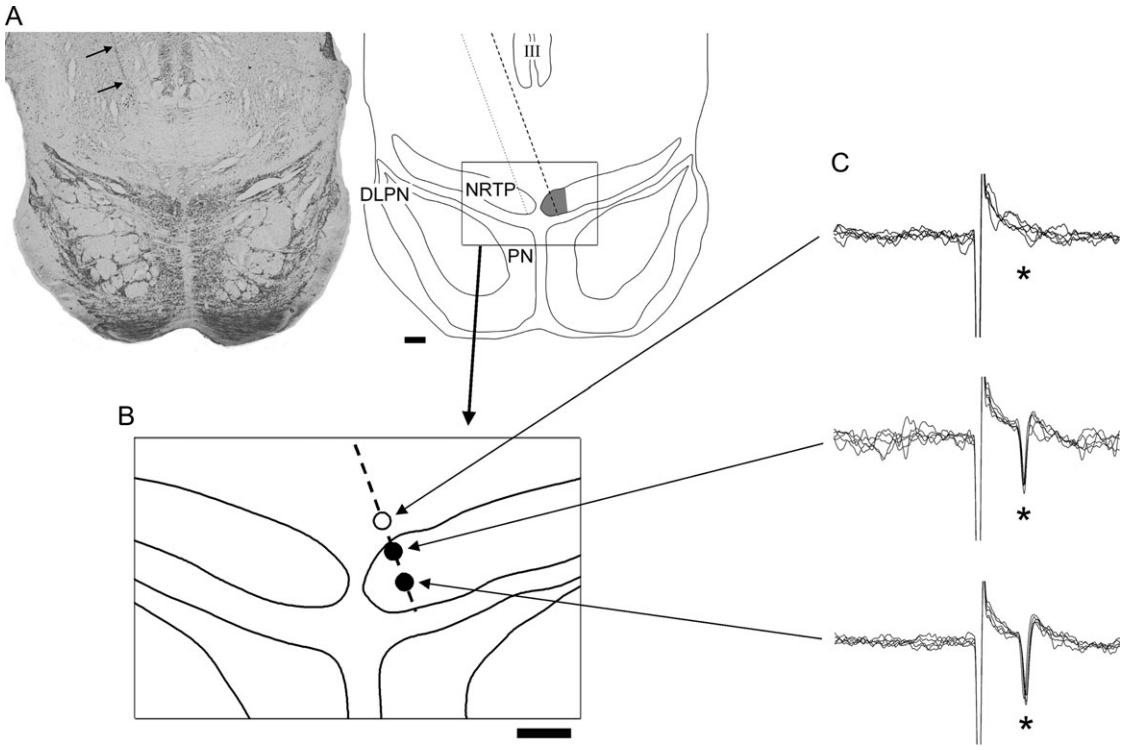

Figure 2. Location of the rNRTP and depth profile of effective stimulation sites for FEF antidromic activation. (*A*) Nissl-stained section and line drawing showing anatomical location of rNRTP region, where SP neurons were recorded. Electrode tracks (e.g., arrows) are visible traveling to the rNRTP region on a 20° angle from a chamber placed on the left side of the head. Borders of rNRTP indicated by the dashed outlined area. Inset drawing shows higher magnification view of the rNRTP region (*B*). Successful antidromic testing sites indicated by filled circles inside the rNRTP. Depths were taken from microdrive readings. (*C*) Representative FEF neuron antidromically activated (asterisk) following stimulation (50 μA) at 2 successful sites in the rNRTP. Stimulation delivered immediately above (500 μm) the rNRTP failed to activate FEF neurons (*C*, top). Five successive trials are overlaid for each stimulation site. Scale bar = 1 mm. III, OMN; PN, pontine nucleus.

individual response profiles of SP-related neurons by using combinations of position, velocity, and acceleration of eye and retinal error motion. Similar procedures have been used with success in other parts of the oculomotor system including the cerebellum, OMNs, the pretectal nucleus of the optic tract (NOT), MST cortex, and pontine nucleus (Shidara et al. 1993; Gomi et al. 1998; Sylvestre and Cullen 1999; Inoue et al. 2000; Das et al. 2001; Takemura and Kawano 2002; Ono et al. 2005). Velocity data were filtered using an 80-point finite impulse response (FIR) digital filter with a passband of 50 Hz, and acceleration data were filtered using an 80-point FIR digital filter with a passband of 30 Hz. The spike density function was also filtered at 50 Hz to reduce the variability in the unit response. Saccades were marked with a cursor on eye velocity traces and were removed. After desaccading, the missing eye data (10- to 50-ms duration) were replaced with a linear fit connecting the pre- and postsaccadic regions of data using custom Matlab routines (Mathworks). Averaged data, taken from at least 10 trials in which the animal performed SP, were then used to identify coefficients in the following model:

$$\mathrm{FR}(t) = A + BE(t+\tau_1) + C\dot{E}(t+\tau_1) + D\ddot{E}(t+\tau_1) + ER(t+\tau_2) + F\dot{R}(t+\tau_2) + G\ddot{R}(t+\tau_2).$$

In the equation described above, $E(t)$ denotes the eye position at time "t," $R(t)$ denotes the retinal error position at time t, and $\mathrm{FR}(t)$ is the estimated value of the unit spike density function at time t. Coefficients in the models are defined by terms A, B, C, D, E, F, and G. Therefore, this model attempts to relate unit response to a combination of eye and retinal error motion parameters. The latency value of the unit response with respect to pursuit onset "τ_1" represents the eye latency and "τ_2" represents the visual latency (unit response following target motion onset). The goodness of fit was determined by calculating a coefficient of determination (CD) or the square of the cross-correlation coefficient between experimentally observed unit data and model estimated fit (Glantz 1987). We calculated a set of coefficients (A–G) and estimated CDs for a series of τ_1 and τ_2 latencies. In our final model, we used coefficients that yielded a maximum CD for specific latency values (e.g., Das et al. 2001; Ono et al. 2005). Retinal error parameters were calculated as the difference between target and eye motion parameters. Because FEF units are generally unresponsive to large velocities, the impulse in target velocity due to differentiation of the step in target position was removed in software prior to presenting the data to the modeling algorithm (e.g., Fig. 4*B*–*E*). Further, target acceleration was assumed as $0°/s^2$ because differentiation of a step in target velocity results in zero steady-state target acceleration (e.g., Fig. 4*B*–*F*) (Das et al. 2001; Ono et al. 2005).

We also calculated partial r^2 values for each component to estimate the relative contribution of eye and retinal error position, velocity, and acceleration to the firing rate of the neurons in FEF. All statistical tests were executed with a significance value of 0.05 unless otherwise specified.

Results

Identified Neurons in FEF–rNRTP Pathway

We delivered ES in rNRTP to test 54 well-isolated neurons in FEF. Of these, 29 neurons in FEF were antidromically activated from rNRTP (Fig. 1*B*,*C*). Median latency between stimulation in the rNRTP and evoked FEF spikes was 1.69 ms (Fig. 1*C*). We found that 20/29 neurons responded during SP tracking of small target spot over a dark background, whereas 9/29 neurons were not modulated during SP testing (Fig. 1*C*) but evinced visual or saccadic sensitivity. We also recorded 25 SP neurons, which were not activated following electrical stimulation of rNRTP (see Discussion).

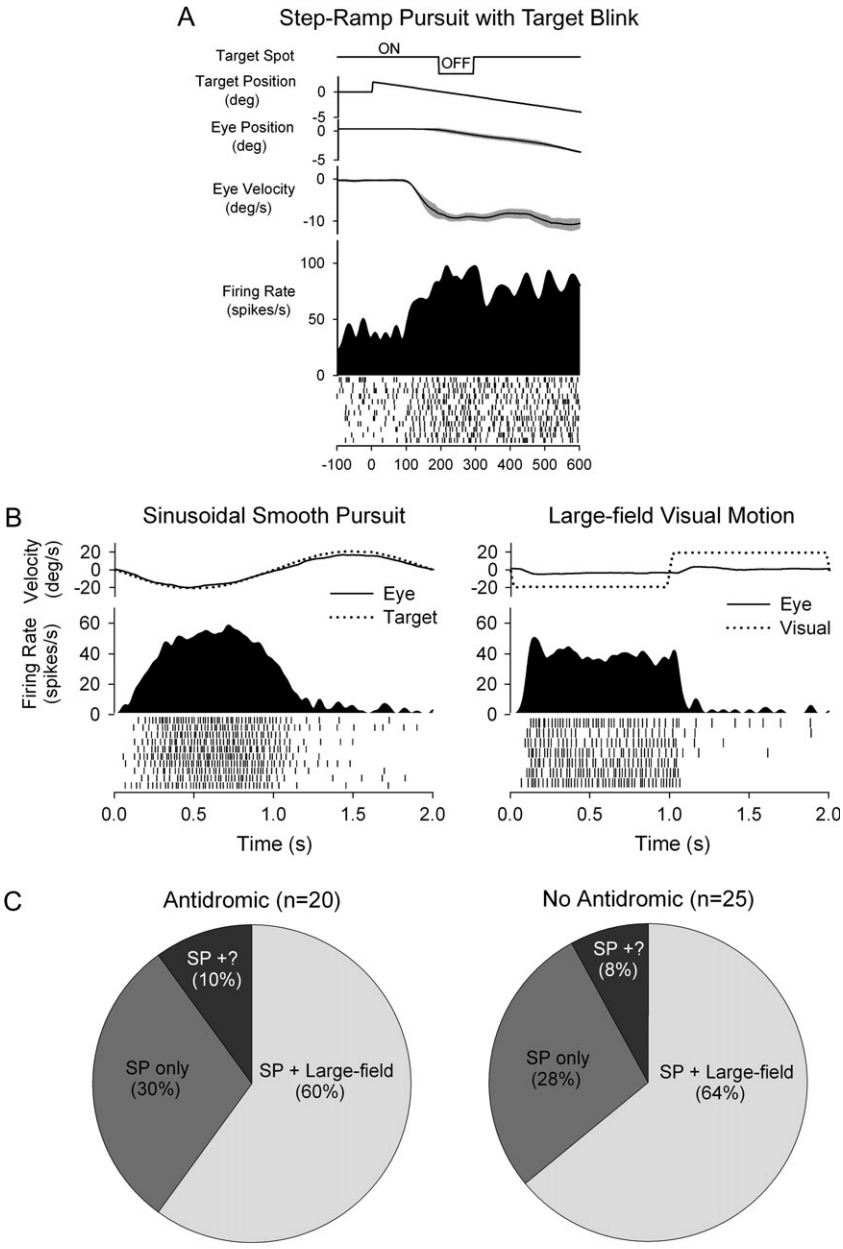

Figure 3. SP and visual sensitivity of FEF neurons. (*A*) Example of FEF neuron tested during step-ramp pursuit with target blink. Response continues during the blink, indicating extraretinal sensitivity. (*B*) Representative neuronal response of FEF neuron during sinusoidal SP tracking at 0.5 Hz ± 10° and visual stimulation with a large-field, constant speed random dot pattern (0.5 Hz ± 10°). This SP-related neuron also showed a visual response at short latency (~65 ms) following the start of leftward visual motion. (*C*) Proportional distributions of large-field visual and SP responses in activated and nonactivated FEF neurons. Isolation was lost on some SP neurons before visual testing during fixation (SP+?).

Figure 4 illustrates the response of a representative FEF neuron that was antidromically activated from rNRTP. This neuron was well modulated during step-ramp tracking with a leftward (contralateral) preference and showed a particularly strong modulation during initial part of step-ramp tracking (Fig. 4*A*). This strong initial modulation could indicate neuronal sensitivity to visual motion or eye acceleration. The model estimation procedure for the unit of Figure 4*A* is shown in Figure 4*B-a–B-b*. Panels (*a–f*) illustrates the components that were used to make up the model. Panel (*g*) illustrates the contribution of each term of the model toward the total fit. Examination of each component of this model (Fig. 4*B*, panel *g*) indicates that eye acceleration contributes most to the unit response during step-ramp tracking, whereas contributions of eye position, eye velocity, and retinal error components were relatively small. The fit obtained using this 6-component model had a CD of 0.93. Unit response lags the onset of target motion by 82 ms and leads the onset of eye motion by an average of 5 ms. We always used the latencies associated with highest CD values to construct our models. Panel (*b*) illustrates that the experimentally derived unit spike density function (orange trace) was fit quite well by the corresponding model (green trace). In contrast, if we removed the eye acceleration contribution, the fit was unsatisfactory. The dependence of FEF neurons on eye acceleration can also be revealed during sinusoidal tracking, where eye motion occurs around different initial orbital positions (see Discussion).

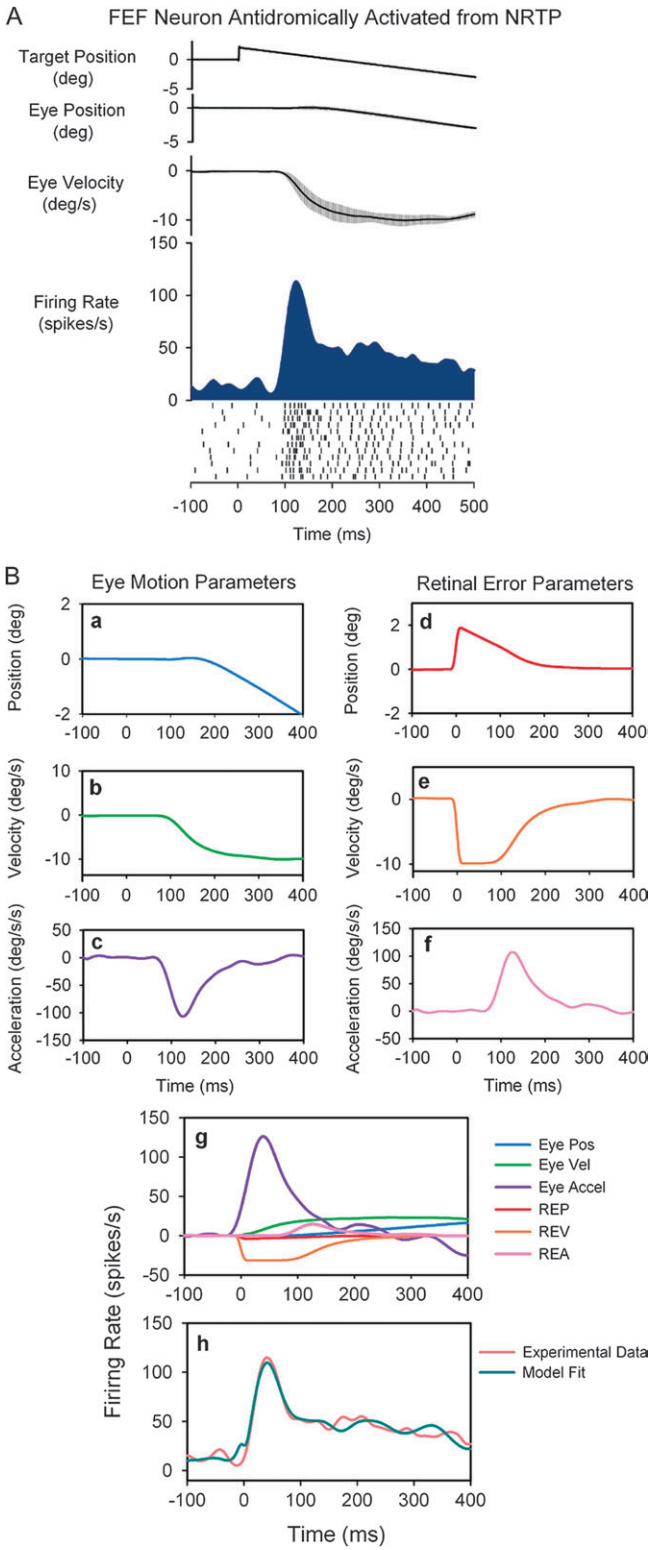

Figure 4. Step-ramp SP response of a representative FEF neuron that was antidromically activated from rNRTP. (*A*) Averaged data from step-ramp trials (10°/s). Traces show horizontal target and eye position, eye velocity, and neuronal activity (spike density and rasters). (*B*) Curve-fitting procedure used to identify model parameters. Individual panels (*a–f*) show the dynamic values of the components that make up the model. (*g*) The relative contributions of the components of the model toward the unit response. (*h*) The observed spike density function and the best fit obtained using the model below. The equation for the corresponding fit: $FR(t) = 10.07 - 5.65E(t-5) - 2.31\dot{E}(t-5) - 1.18\ddot{E}(t-5) - 2.14R(t+82) + 3.18\dot{R}(t+82) + 0.14\ddot{R}(t+82)$. The neuron was most sensitive to eye acceleration.

Figure 5 illustrates a FEF neuron that was not activated following ES of rNRTP. This neuron was well modulated during step-ramp tracking with a leftward (contralateral) direction preference. Examination of Figure 5*A* shows that the neuron did not have the strong initial transient response component at pursuit initiation. The model estimation procedure for this unit is shown in Figure 5*B*. The fit obtained using this 6-component model had a CD of 0.97. Unit response lags the onset of target motion by 98 ms and leads onset of eye motion by 2 ms. Examination of Figure 5*B-g* indicates that the neuron is most sensitive to eye velocity during step-ramp tracking, with significantly smaller contributions from eye position, eye acceleration, and retinal error components. Figure 5*h* shows that the experimental data (orange trace) were well fit by the derived model (green trace).

Model Testing

The 6-component model provided a good fit to all the experimentally derived data in FEF (CD = 0.75 ± 0.15, n = 45). We determined the distribution of partial r^2 values for eye and retinal error position, velocity, and acceleration to show the differential sensitivity of each FEF neuron (antidromically activated or not activated) to each motion component. These partial r^2 are plotted in Figure 6*A*. The majority of FEF neurons antidromically activated following rNRTP stimulation have the largest contributions from eye acceleration compared with eye position, velocity, or retinal error motion during step-ramp tracking (Fig. 6*A*, red circles). In contrast, we found that FEF neurons not activated have a distribution of partial r^2 values indicating larger contributions from eye velocity rather than acceleration during step-ramp tracking (Fig. 6*A*, blue circles). Median partial r^2 values for antidromically activated neurons are higher for eye acceleration (0.21, n = 20) than eye velocity (0.06, n = 20), eye position (0.04, n = 20), or retinal error components (P < 0.001, 1-way analysis of variance (ANOVA) on ranks; Fig. 6*B*). In contrast, median partial r^2 values for neurons not activated indicate that eye velocity (0.18, n = 25) makes a larger contribution than eye position (0.06, n = 25), acceleration (0.05, n = 25), or retinal error components (P < 0.001, 1-way ANOVA on ranks; Fig. 6*C*).

We compared latencies of the unit responses with respect to pursuit onset for antidromically activated and nonactivated neurons. We also examined the CDs obtained using the 6-component model for these same 2 groups. We examined the estimates of latency as calculated for best fits of our models. The distribution and median values (26.5 ms, n = 20) of latencies for antidromically activated neurons was similar to that of nonactivated neurons (median values = 25.0 ms, n = 25). The distribution of CDs and median values for antidromically activated neurons (0.79, n = 20) was similar to values found for nonactivated (median values = 0.78, n = 25).

For comparative purposes, we show the results of using only eye parameters (3-component model) compared with our 6-component models, which include retinal error terms. The actual FEF neuronal response (dotted lines) during step-ramp tracking for neurons with strong eye acceleration (Fig. 7*A*, left, CD = 0.86) or eye velocity (Fig. 7*A*, right, CD = 0.81) could be well fit using only eye parameters in our model (red traces). However, the 6-component models produced better fits (Fig. 7*A*, green traces). In Figure 7*B*, we plot the CDs for 6-component model (ordinate) against an eye only (position,

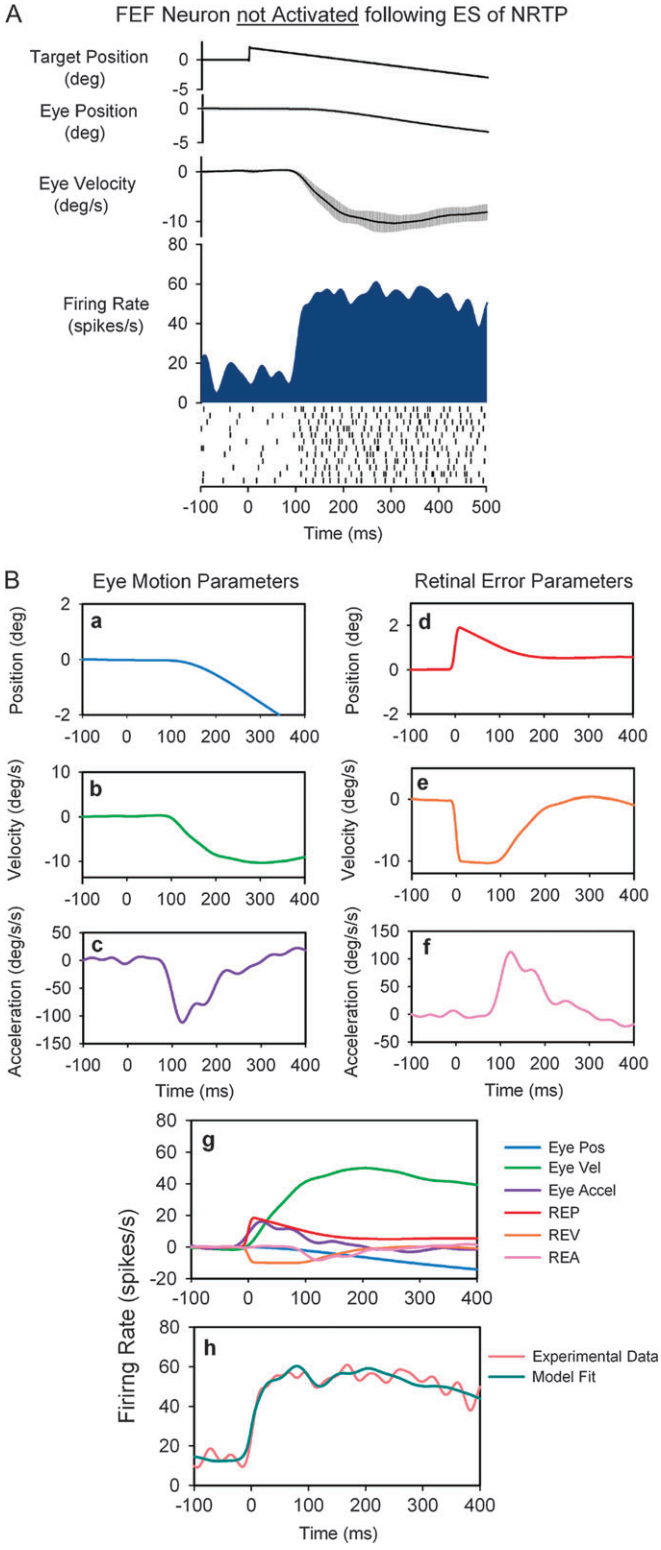

Figure 5. SP response of a representative FEF neuron not activated following electrical stimulation of rNRTP. See Figure 4 for description of panels. The equation for the best fit in (*h*): $FR(t) = 14.26 + 5.19E(t-2) - 4.26\dot{E}(t-2) + 0.02\ddot{E}(t-2) + 21.26R(t+98) + 1.15\dot{R}(t+98) - 0.05\ddot{R}(t+98)$. The neuron was most sensitive to eye speed.

velocity, and acceleration) model. Most of our FEF (antidromically activated and nonactivated) neurons fall above the unity line indicating improved fits when retinal error terms are included. In the Discussion, we consider some potential problems of codependency of different parameters in these models.

In a previous study (Ono et al. 2005), we showed that SP-related neurons in rNRTP were most sensitive to eye acceleration. In Figure 8, we show examples of FEF (Fig. 8*A*) and rNRTP (Fig. 8*B*) neurons during step-ramp tracking and their partial r^2 values obtained in our modeling studies (Fig. 8*C*). Although the population of antidromically activated FEF and rNRTP neurons is small, there is considerable overlap in the distributions with respect to eye motion parameters. Eye acceleration provides the largest contribution to FEF and rNRTP SP activity during step-ramp tracking.

Discussion

SP is a volitional behavior supported by a network of cerebral cortical areas comprising the cortical pursuit system (for review, see Krauzlis 2004). Anatomical studies show that different areas in the cortical pursuit system provide parallel projections to brain stem regions, some of which send signals to the oculomotor cerebellum for SP control. However, there is little direct evidence available about the information provided by a given cortical area to specific brain stem targets involved in SP. Important cortical–brain stem targets for controlling SP metrics include the NRTP, DLPN, and pretectal NOT. Other cortical projections such as those involving the basal ganglia and superior colliculus may play a role in higher order properties of SP such as target selection and learning (for reviews, see Krauzlis 2004; Leigh and Zee 2006; Utter and Basso 2008).

A major goal of our current study was to characterize SP-related information provided by the FEF to the rNRTP. Antidromic activation provides the most powerful tool for addressing this question because projection neurons are positively identified and characterized. Therefore, we used ES delivered in rNRTP to antidromically activate FEF neurons. We applied a modeling procedure employing multiple linear regression to estimate the relative contributions of different eye and visual motion parameters (acceleration, velocity, and position) to neuronal responses. A multivariate description could be appropriate because SP-related FEF neurons evince multiple sensitivities. We found that SP-related FEF neurons that project to rNRTP are most strongly related to eye motion (acceleration and velocity). This sensitivity and other findings, discussed below, support the suggestion that the FEF plays an important role in generating volitional SP.

Our approach has some important constraints and advantages. First, we may not be successful in antidromically activating all the layer-5 FEF neurons that actually project to rNRTP. This could be due to our use of low currents (<200 μA) or nonoptimal placement of our stimulating electrodes in rNRTP. However, our depth profiles of effective stimulus sites indicate that our stimulus electrodes were well placed. Our recording and stimulation sites in the rNRTP appear to coincide with the locations of patchy anatomically defined projections from FEF reported in other studies (for review, see Thier and Möck 2006). Nevertheless, we cannot be sure that our FEF recording electrode and NRTP stimulating electrodes were always in optimal register. Second, our modeling and experimental approach considers only parameters related to visual or eye motion per se and not higher

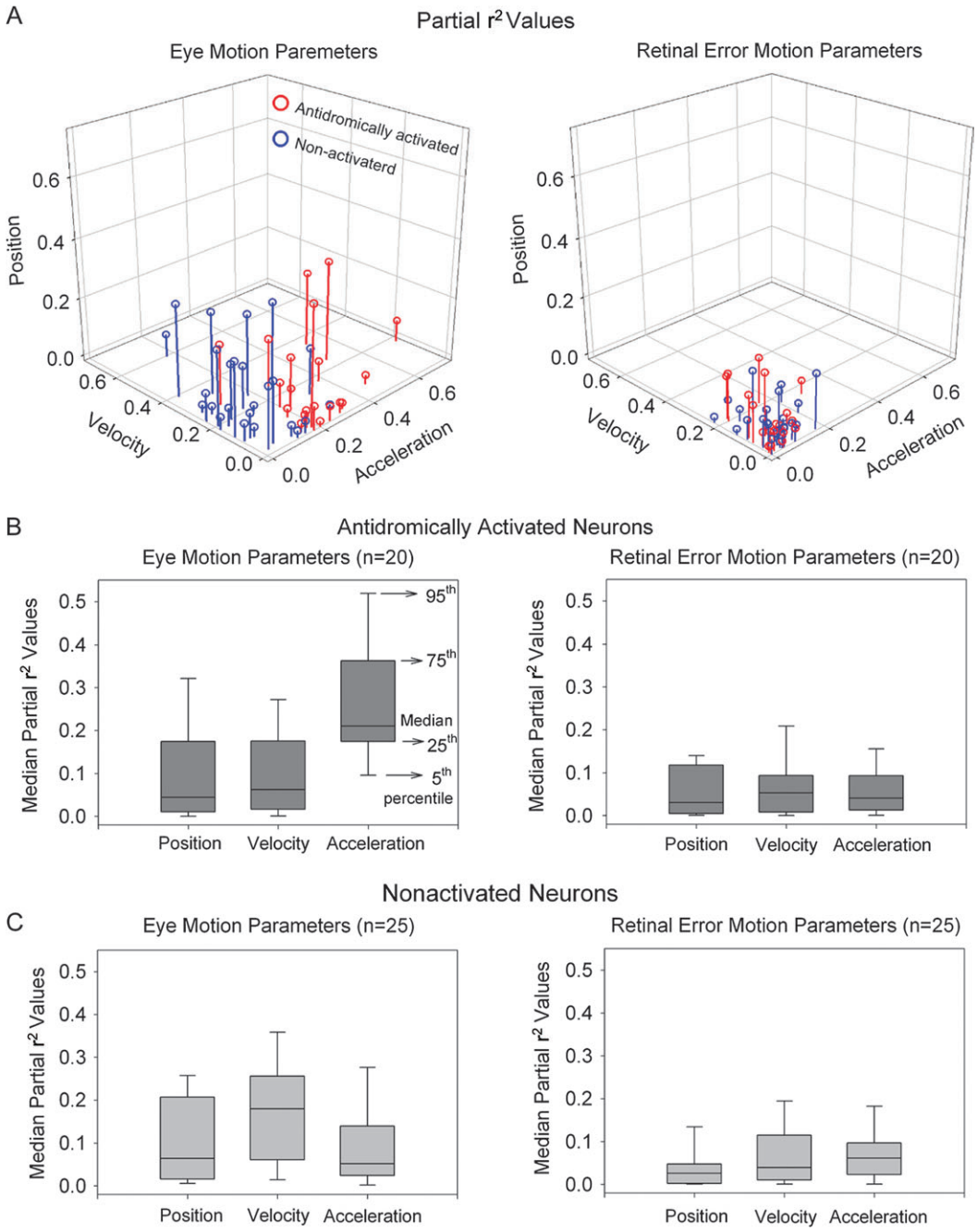

Figure 6. Comparison of partial r^2 values between eye (*A*, left panel) and retinal error (*A*, right panel) position, velocity, and acceleration parameters for each FEF neuron antidromically activated (red symbols) or not activated (blue symbols) following electrical stimulation of rNRTP. (*B*) Median partial r^2 values of eye motion (left panel) and retinal error motion parameters (right panel) for neurons antidromically activated from rNRTP. Eye acceleration parameters show larger partial r^2 values than eye position and velocity parameters, indicating the relative importance of eye acceleration. Retinal error motion parameters show relatively smaller contributions than eye motion parameters. (*C*) Median partial r^2 values of eye motion (left panel) and retinal error motion parameters (right panel) in neurons not activated following electrical stimulation of rNRTP. Eye velocity parameter shows larger partial r^2 values than eye position and acceleration parameters, indicating the relative importance of eye velocity.

order components such as attention or prediction that might also modulate neuronal response (for reviews, see Fukushima 2003; Schall 2004). Furthermore, we have purposefully confined our studies to SP in head-restrained monkeys. Some of our antidromically activated neurons may play a role in gaze as described by others (for reviews, see Fukushima 2003; Knight and Fuchs 2007). In any case, our approach has the advantage of allowing us to address a fundamental gap in our knowledge of information processing at a node in the cortical pursuit system and distribution of cortical signals to specific brain stem targets.

Differential Signal Processing in the Cortical Pursuit System

The FEF receives projections from other frontal and parietal cortical areas. Evidences from single-unit recording and lesion studies indicate significant differences in SP-related functions of different cortical areas. For example, lesions placed in the cortical

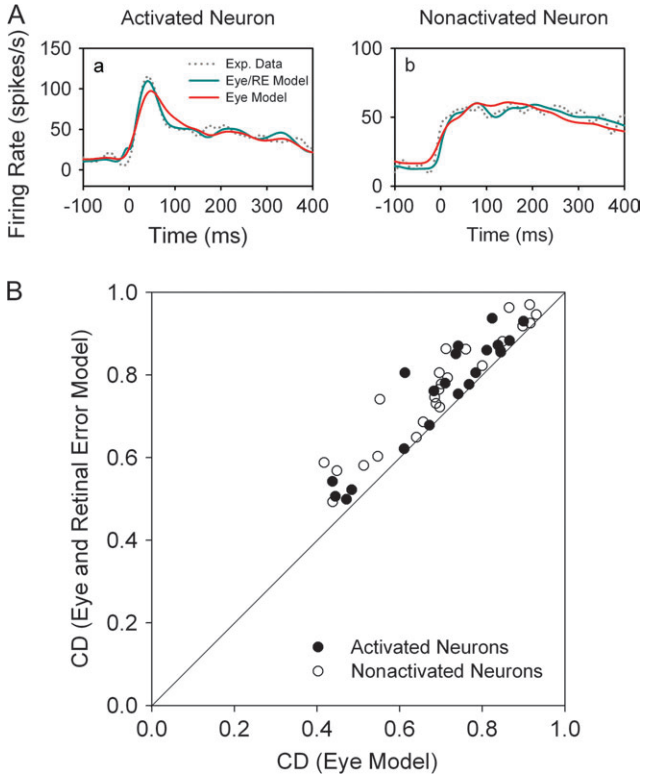

Figure 7. Comparison of CDs obtained using 6-component (eye and retinal error motion) model versus CDs obtained using 3-component (eye motion) models. (*A*) The observed spike density function (dotted lines) and the best fit obtained using 6-component (green traces) or 3-component (red traces) models in representative antidromically activated (*a*) and nonactivated (*b*) neurons. (*B*) Pairwise comparisons of CDs taken from 6-component and 3-component models of antidromically activated (filled circles) and nonactivated (open circles) neuronal responses.

visual motion processing areas MT and MST produced retinotopic and directional deficits in SP, respectively (Newsome et al. 1985; Dursteler et al. 1987). Some neurons in lateral (MSTl) and dorsal aspects of MST (MSTd) carry extraretinal signals related to SP eye movements. MSTd neuronal discharge often follows the onset of the eye movement by up to 100 ms (Newsome et al. 1988; Squatrito and Maioli 1996; Akao et al. 2005; Ono and Mustari 2006), perhaps reflecting efference copy information.

Both MT and MST have reciprocal connections with the FEF region (for review, see Lynch and Tian 2006). Single-unit studies have shown that FEF neurons have appropriate response properties for initiating and maintaining SP eye movement (MacAvoy et al. 1991; Gottlieb et al. 1994; Tanaka and Fukushima 1998). The majority of FEF neurons begin their response before the onset of pursuit, and they contribute to the initiation of pursuit, which is characterized by high retinal slip and eye acceleration (e.g., Gottlieb et al. 1994; for review, see Fukushima 2003). Eye velocity–sensitive neurons in FEF could be associated with roles in maintenance of steady-state eye velocity and gain control of SP (see Tanaka and Lisberger 2002; for reviews, see Nuding et al. 2008). Lesions of FEF are associated with defective predictive and visually guided SP (Shi et al. 1988; Keating 1991; MacAvoy et al. 1991). Electrical stimulation delivered in FEF produces enhancement of both the direction and the gain of pursuit (Tanaka and Lisberger 2002). These FEF influences on SP are likely mediated by projections traveling through the pontine nuclei.

Cortical–Pontine Projections and Antidromic Studies

Anatomical studies have shown that FEF projects strongly to the NRTP and less so to the DLPN (e.g., Distler et al. 2002; for reviews, see Lynch and Tian 2006; Thier and Möck 2006). The NRTP and DLPN provide primary projections to oculomotor vermis (lobules VI and VII) and paraflocculus (Brodal 1980, 1982). Lesion studies involving oculomotor regions of the cerebellum produce specific deficits in SP. For example, Takagi et al. (2000) have demonstrated that the lesions of oculomotor vermis (lobules VI and VII) produce the most significant deficits in the open loop (initiation) rather than closed loop (maintenance) portions of SP. Recent single-unit recording studies show that neurons in oculomotor vermis respond with appropriate lead times to play a role in initiation of SP and vergence (Nitta et al. 2007). These authors also showed that focal injections of muscimol in oculomotor vermis resulted in impairment of initiation of SP and vergence.

Our modeling and antidromic activation studies support the suggestion that the FEF is a likely source of acceleration-related signals (essential for initiating SP) found in the rNRTP (Suzuki et al. 2003; Ono et al. 2004). For example, we have found that FEF and rNRTP have overlapping eye motion sensitivities (e.g., Fig. 8). In contrast, we have not found evidence of neurons with strong eye acceleration sensitivity in cortical area MST (Ono and Mustari 2006; Nuding et al. 2008), DLPN (Ono et al. 2004, 2005), or NOT (Das et al. 2001). By using the same modeling approach for neurons at different nodes in the SP system, we are able to compare and contrast eye and retinal motion sensitivity associated with the same pursuit behavior. For example, NOT neurons are sensitive to foveal/parafoveal visual motion during SP but show no eye motion sensitivity per se (Das et al. 2001). Modeling NOT neurons with retinal error terms alone is highly effective. In contrast, SP neurons in the DLPN and NRTP show both eye and retinal motion sensitivity. In these areas, models that include both eye motion and retinal motion components are most effective. In our current studies, we sometimes used large-field visual motion stimulation (Fig. 3*B,C*) to reveal FEF visual sensitivity. Large-field visual stimuli may activate peripheral visual receptive fields that do not include strong representation of the fovea. In such cases, a 3-component eye model (Fig. 7) may be most appropriate.

A potential concern in our modeling study is whether visual and eye motion response components (position, velocity, and acceleration) are acting independently. In closed loop tracking, like that studied here, eye motion will produce foveal/parafoveal visual motion correlated with eye movement. Examination of successive trials for visual motion or pursuit (Figs 3–5) shows that there is little variation in visual or eye onset latencies, across trials. Therefore, at least some separability exists between visual and eye motion components because of latency differences. Similarly, target blink testing indicates that most SP units have eye motion (extraretinal) sensitivity independent of actual retinal image motion. Nevertheless, modeling studies using both eye and retinal error components should be viewed as providing estimates of response sensitivities not absolute values. Partial r^2 values provide further estimates of likely contributions of various components to neuronal response.

We suggest that neurons in the FEF–rNRTP pathway carry signals that could play a primary role in initiation and a secondary role in maintaining SP. We found a significant

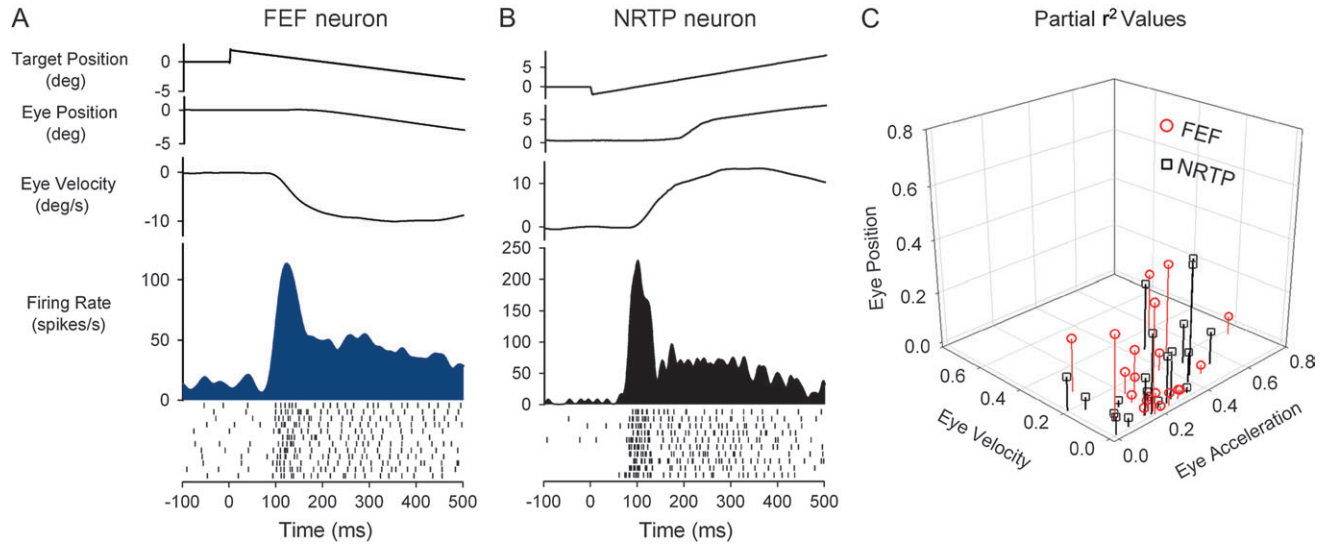

Figure 8. Comparison of neuronal response dynamics for representative FEF (conventions as in Figure 3) and rNRTP (Ono et al. 2005) SP neurons during step-ramp tracking. Response of antidromically activated FEF SP neuron (*A*) and rNRTP SP neuron (*B*). Both neurons show a strong transient responses during SP initiation. (*C*) Partial r^2values for SP neurons in the rNRTP (Ono et al. 2005) and in FEF (antidromically activated from rNRTP). Both populations show considerable overlap with a trend toward most sensitivity to eye acceleration.

proportion of FEF neurons that were not activated following electrical stimulation of rNRTP. This is expected because only layer-5 neurons project to the brain stem. Some of our nonactivated neurons may project to other pontine, brain stem, or cortical regions (e.g., MST). For example, we expect that FEF neurons with eye velocity sensitivity may project preferentially to the DLPN. We actually know very little about whether different functional unit types of FEF neurons are located in different cortical layers. Antidromic activation of FEF neurons from different brain stem and cortical areas would help address this gap in our knowledge.

Signal Integration in Pontine Nuclei

One of the most important unresolved questions regarding rNRTP and basilar pontine function, in general, is whether these areas simply relay signals from cortex to the cerebellum or whether significant processing and signal integration occurs in the pontine nuclei per se. By performing antidromic and modeling studies, we were able to compare the properties of neurons in FEF and rNRTP for evidence of signal transformation. Our published modeling studies of SP neurons in rNRTP showed that they were most sensitive to eye acceleration (Ono et al. 2005). We found that FEF and rNRTP neurons have largely overlapping eye and visual motion sensitivities (see Fig. 8). Therefore, we suggest that rNRTP faithfully relays FEF signals to the cerebellar vermis. We still do not know if signals from different cortical areas such as SEF, FEF, and MST are integrated in the NRTP, DLPN, or in distal sites. Studies by Suh et al. (2000) have shown that neurons in ventral paraflocculus, which receive strong projections from DLPN, carry signals strongly related to eye motion (velocity) during SP. Ventral paraflocculus neurons also evince signals related to prediction or possibly acceleration in certain paradigms.

There is considerable specificity in the cortical projections to DLPN and rNRTP (Glickstein et al. 1980, 1994; May and Andersen 1986; Giolli et al. 2001; Distler et al. 2002; for review, see Thier and Möck 2006) with FEF providing a stronger input to rNRTP, MST to DLPN, and MT to DLPN and NOT (Distler et al. 2002). Single-unit recording (Suzuki and Keller 1984; Mustari et al. 1988; Thier et al. 1988; Suzuki et al. 1990; Suzuki et al. 2003; Ono et al. 2004, 2005) and lesion studies (May et al. 1988; Ono et al. 2003) demonstrate that NRTP and DLPN neurons carry complimentary signals essential for initiation and maintenance of SP. There are also DLPN neurons that are most sensitive to visual motion per se with little pursuit-related response (Suzuki and Keller 1984; Mustari et al. 1988; Thier et al. 1988; Suzuki et al. 1990; Ono et al. 2005). Unilateral DLPN inactivation produces consistent deficits in the ability to generate and maintain SP in the ipsilesional direction. Similarly, rNRTP lesions produce deficits in the initiation of pursuit and gaze (Suzuki et al. 1999). Recently, we used multiple linear regression modeling to demonstrate that most SP neurons in the DLPN encode eye motion with smaller contributions from retinal error motion. In contrast, rNRTP neurons are most sensitive to eye acceleration (Ono et al. 2005).

Conclusion and Future Studies

In conclusion, we have provided evidence that FEF neurons projecting to rNRTP carry information strongly related to eye motion including eye acceleration and velocity. It is possible that some of the FEF neurons that were not activated following rNRTP stimulation project to other targets such as the DLPN. By using the same modeling approach in rNRTP, DLPN, NOT, MST, and FEF, we have been able to directly compare and contrast SP-related signals in all these areas. It is important to note that neurons with high degrees of eye acceleration sensitivity are not found in the DLPN or MST. Our findings support the suggestion that FEF–rNRTP pathway carries signals that could play a primary role in initiation of SP. Because of the substantial overlap between neuronal response properties of antidromically activated FEF neurons and rNRTP SP neurons, it is possible that FEF signals are relayed to the cerebellum with little additional processing. Further studies that involve electrical stimulation of both DLPN and NRTP may help resolve

whether the FEF sends the same or different signals to specific channels of the cortical–ponto–cerebellar system.

Funding

National Institutes of Health Grants. (National Eye Institute, EY13308; RR00165).

Notes

We wish to acknowledge the expert assistance provided by Mrs Tracey Fountain and Dr Katia C. Vitorello. *Conflict of Interest*: None declared.

Address correspondence to email: mjmustar@rmy.emory.edu.

References

Akao T, Mustari MJ, Fukushima J, Kurkin S, Fukushima K. 2005. Discharge characteristics of pursuit neurons in MST during vergence eye movements. J Neurophysiol. 93:2415–2434.

Brodal P. 1980. The cortical projection to the nucleus reticularis tegmenti pontis in the rhesus monkey. Exp Brain Res. 38:19–27.

Brodal P. 1982. Further observations on the cerebellar projections from the pontine nuclei and the nucleus reticularis tegmenti pontis in the rhesus monkey. J Comp Neurol. 204:44–55.

Bruce CJ, Goldberg ME, Bushnell MC, Stanton GB. 1985. Primate frontal eye fields. II. Physiological and anatomical correlates of electrically evoked eye movements. J Neurophysiol. 54:714–734.

Das VE, Economides JR, Ono S, Mustari MJ. 2001. Information processing by parafoveal cells in the primate nucleus of the optic tract. Exp Brain Res. 140:301–310.

Distler C, Mustari MJ, Hoffmann KP. 2002. Cortical projections to the nucleus of the optic tract and dorsal terminal nucleus and to the dorsolateral pontine nucleus in macaques: a dual retrograde tracing study. J Comp Neurol. 444:144–158.

Drew AS, van Donkelaar P. 2007. The contribution of the human FEF and SEF to smooth pursuit initiation. Cereb Cortex. 17:2618–2624.

Dursteler MR, Wurtz RH, Newsome WT. 1987. Directional pursuit deficits following lesions of the foveal representation within the superior temporal sulcus of the macaque monkey. J Neurophysiol. 57:1262–1287.

Fuchs AF, Robinson DA. 1966. A method for measuring horizontal and vertical eye movement chronically in the monkey. J Appl Physiol. 21:1068–1070.

Fukushima K. 2003. Frontal cortical control of smooth-pursuit. Curr Opin Neurobiol. 13:647–654.

Giolli RA, Gregory KM, Suzuki DA, Blanks RH, Lui F, Betelak KF. 2001. Cortical and subcortical afferents to the nucleus reticularis tegmenti pontis and basal pontine nuclei in the macaque monkey. Vis Neurosci. 18:725–740.

Glantz SA. 1987. Primer of bio-statistics. 4th ed. New York: McGraw Hill.

Glickstein M, Cohen JL, Dixon B, Gibson A, Hollins M, Labossiere E, Robinson F. 1980. Corticopontine visual projections in macaque monkeys. J Comp Neurol. 190:209–229.

Glickstein M, Gerrits N, Kralj-Hans I, Mercier B, Stein J, Voogd J. 1994. Visual pontocerebellar projections in the macaque. J Comp Neurol. 349:51–72.

Gomi H, Shidara M, Takemura A, Inoue Y, Kawano K, Kawato M. 1998. Temporal firing patterns of Purkinje cells in the cerebellar ventral paraflocculus during ocular following responses in monkeys. I. Simple spikes. J Neurophysiol. 80:818–831.

Gottlieb JP, Bruce CJ, MacAvoy MG. 1993. Smooth eye movements elicited by microstimulation in the primate frontal eye field. J Neurophysiol. 69:786–799.

Gottlieb JP, MacAvoy MG, Bruce CJ. 1994. Neural responses related to smooth-pursuit eye movements and their correspondence with electrically elicited smooth eye movements in the primate frontal eye field. J Neurophysiol. 72:1634–1653.

Huerta MF, Krubitzer LA, Kaas JH. 1986. Frontal eye field as defined by intracortical microstimulation in squirrel monkeys, owl monkeys, and macaque monkeys: I. Subcortical connections. J Comp Neurol. 253:415–439.

Inoue Y, Takemura A, Kawano K, Mustari MJ. 2000. Role of the pretectal nucleus of the optic tract in short-latency ocular following responses in monkeys. Exp Brain Res. 131:269–281.

Judge SJ, Richmond BJ, Chu FC. 1980. Implantation of magnetic search coils for measurement of eye position: an improved method. Vision Res. 20:535–538.

Keating EG. 1991. Frontal eye field lesions impair predictive and visually-guided pursuit eye movements. Exp Brain Res. 86:311–323.

Keating EG. 1993. Lesions of the frontal eye field impair pursuit eye movements, but preserve the predictions driving them. Behav Brain Res. 53:91–104.

Keller EL, Heinen SJ. 1991. Generation of smooth-pursuit eye movements: neuronal mechanisms and pathways. Neurosci Res. 11:79–107.

Knight TA, Fuchs AF. 2007. Contribution of the frontal eye field to gaze shifts in the head-unrestrained monkey: effects of microstimulation. J Neurophysiol. 97:618–634.

Komatsu H, Wurtz RH. 1988. Relation of cortical areas MT and MST to pursuit eye movements. III. Interaction with full-field visual stimulation. J Neurophysiol. 60:621–644.

Krauzlis RJ. 2004. Recasting the smooth pursuit eye movement system. J Neurophysiol. 91:591–603.

Kunzle H, Akert K. 1977. Efferent connections of cortical, area 8 (frontal eye field) in Macaca fascicularis. A reinvestigation using the autoradiographic technique. J Comp Neurol. 173:147–164.

Leigh RJ, Zee DS. 2006. The neurology of eye movements. 4th ed. New York: Oxford University Press.

Lynch JC. 1987. Frontal eye field lesions in monkeys disrupt visual pursuit. Exp Brain Res. 68:437–441.

Lynch JC, Tian JR. 2006. Cortico-cortical networks and cortico-subcortical loops for the higher control of eye movements. Prog Brain Res. 151:461–501.

MacAvoy MG, Gottlieb JP, Bruce CJ. 1991. Smooth-pursuit eye movement representation in the primate frontal eye field. Cereb Cortex. 1:95–102.

Maunsell JH, Newsome WT. 1987. Visual processing in monkey extrastriate cortex. Annu Rev Neurosci. 10:363–401.

May JG, Andersen RA. 1986. Different patterns of corticopontine projections from separate cortical fields within the inferior parietal lobule and dorsal prelunate gyrus of the macaque. Exp Brain Res. 63:265–278.

May JG, Keller EL, Suzuki DA. 1988. Smooth-pursuit eye movement deficits with chemical lesions in the dorsolateral pontine nucleus of the monkey. J Neurophysiol. 59:952–977.

Mitchell JF, Sundberg KA, Reynolds JH. 2007. Differential attention-dependent response modulation across cell classes in macaque visual area V4. Neuron. 55:131–141.

Morrow MJ. 1996. Craniotopic defects of smooth pursuit and saccadic eye movement. Neurology. 46:514–521.

Morrow MJ, Sharpe JA. 1990. Cerebral hemispheric localization of smooth pursuit asymmetry. Neurology. 40:284–292.

Mustari MJ, Fuchs AF, Wallman J. 1988. Response properties of dorsolateral pontine units during smooth pursuit in the rhesus macaque. J Neurophysiol. 60:664–686.

Mustari MJ, Tusa RJ, Burrows AF, Fuchs AF, Livingston CA. 2001. Gaze-stabilizing deficits and latent nystagmus in monkeys with early-onset visual deprivation: role of the pretectal not. J Neurophysiol. 86:662–675.

Newsome WT, Wurtz RH, Dursteler MR, Mikami A. 1985. Deficits in visual motion processing following ibotenic acid lesions of the middle temporal visual area of the macaque monkey. J Neurosci. 5:825–840.

Newsome WT, Wurtz RH, Komatsu H. 1988. Relation of cortical areas MT and MST to pursuit eye movements. II. Differentiation of retinal from extraretinal inputs. J Neurophysiol. 60:604–620.

Nitta T, Akao T, Kurkin S, Fukushima K. 2007. Involvement of the cerebellar dorsal vermis in vergence eye movements in monkeys. Cereb Cortex. 18:1042–1057.

Nuding U, Ono S, Mustari MJ, Buttner U, Glasauer S. 2008. A theory of the dual pathways for smooth pursuit based on dynamic gain control. J Neurophysiol. 99:2798–2808.

Ono S, Das VE, Economides JR, Mustari MJ. 2005. Modeling of smooth pursuit-related neuronal responses in the DLPN and NRTP of the rhesus macaque. J Neurophysiol. 93:108–116.
Ono S, Das VE, Mustari MJ. 2003. Role of the dorsolateral pontine nucleus in short-term adaptation of the horizontal vestibuloocular reflex. J Neurophysiol. 89:2879–2885.
Ono S, Das VE, Mustari MJ. 2004. Gaze-related response properties of DLPN and NRTP neurons in the rhesus macaque. J Neurophysiol. 91:2484–2500.
Ono S, Mustari MJ. 2006. Extraretinal signals in MSTd neurons related to volitional smooth pursuit. J Neurophysiol. 96:2819–2825.
Rashbass C. 1961. The relationship between saccadic and smooth tracking eye movements. J Physiol. 159:326–338.
Richmond BJ, Optican LM, Podell M, Spitzer H. 1987. Temporal encoding of two-dimensional patterns by single units in primate inferior temporal cortex. I. Response characteristics. J Neurophysiol. 57:132–146.
Schall JD. 2004. On the role of frontal eye field in guiding attention and saccades. Vision Res. 44:1453–1467.
Shi D, Friedman HR, Bruce CJ. 1988. Deficits in smooth-pursuit eye movements after muscimol inactivation within the primate's frontal eye field. J Neurophysiol. 80:458–464.
Shidara M, Kawano K, Gomi H, Kawato M. 1993. Inverse-dynamics model eye movement control by Purkinje cells in the cerebellum. Nature. 365:50–52.
Shook BL, Schlag-Rey M, Schlag J. 1990. Primate supplementary eye field: I. Comparative aspects of mesencephalic and pontine connections. J Comp Neurol. 301:618–642.
Squatrito S, Maioli MG. 1996. Gaze field properties of eye position neurones in areas MST and 7a of the macaque monkey. Vis Neurosci. 13:385–398.
Suh M, Leung HC, Kettner RE. 2000. Cerebellar flocculus and ventral paraflocculus Purkinje cell activity during predictive and visually driven pursuit in monkey. J Neurophysiol. 84:1835–1850.
Suzuki DA, Keller EL. 1984. Visual signals in the dorsolateral pontine nucleus of the alert monkey: their relationship to smooth-pursuit eye movements. Exp Brain Res. 53:473–478.
Suzuki DA, May JG, Keller EL, Yee RD. 1990. Visual motion response properties of neurons in dorsolateral pontine nucleus of alert monkey. J Neurophysiol. 63:37–59.
Suzuki DA, Yamada T, Hoedema R, Yee RD. 1999. Smooth-pursuit eye-movement deficits with chemical lesions in macaque nucleus reticularis tegmenti pontis. J Neurophysiol. 82:1178–1186.
Suzuki DA, Yamada T, Yee RD. 2003. Smooth-pursuit eye-movement-related neuronal activity in macaque nucleus reticularis tegmenti pontis. J Neurophysiol. 89:2146–2158.
Sylvestre PA, Cullen KE. 1999. Quantitative analysis of abducens neuron discharge dynamics during saccadic and slow eye movements. J Neurophysiol. 82:2612–2632.
Takagi M, Zee DS, Tamargo RJ. 2000. Effects of lesions of the oculomotor cerebellar vermis on eye movements in primate: smooth pursuit. J Neurophysiol. 83:2047–2062.
Takemura A, Kawano K. 2002. Sensory-to-motor processing of the ocular-following response. Neurosci Res. 43:201–206.
Tanaka M, Fukushima K. 1998. Neuronal responses related to smooth pursuit eye movements in the periarcuate cortical area of monkeys. J Neurophysiol. 80:28–47.
Tanaka M, Lisberger SG. 2001. Regulation of the gain of visually guided smooth-pursuit eye movements by frontal cortex. Nature. 409:191–194.
Tanaka M, Lisberger SG. 2002. Enhancement of multiple components of pursuit eye movement by microstimulation in the arcuate frontal pursuit area in monkeys. J Neurophysiol. 87:802–818.
Thier P, Koehler W, Buettner UW. 1988. Neuronal activity in the dorsolateral pontine nucleus of the alert monkey modulated by visual stimuli and eye movements. Exp Brain Res. 70:496–512.
Thier P, Möck M. 2006. The oculomotor role of the pontine nuclei and the nucleus reticularis tegmenti pontis. Prog Brain Res. 151:293–320.
Tian JR, Lynch JC. 1996. Functionally defined smooth and saccadic eye movement subregions in the frontal eye field of Cebus monkeys. J Neurophysiol. 76:2740–2753.
Utter AA, Basso MA. 2008. The basal ganglia: an overview of circuits and function. Neurosci Biobehav Rev. 32:333–342.